Absorption of Ultra-Intense Laser Pulses

S. C. Wilks, W. L. Kruer, M. Tabak, and A. B. Langdon
University of California, Lawrence Livermore National Laboratory, P.O. Box 808, Livermore, California 94550
(Received 2 March 1992)

We use simulations to investigate the interaction of ultra-intense laser pulses with a plasma. With an intensity greater than 10^{18} W/cm^2, these pulses have a pressure greater than 10^3 Mbar and drive the plasma relativistically. Hole boring by the light beam is a key feature of the interaction. We find substantial absorption into heated electrons with a characteristic temperature of order the ponderomotive potential. Other effects include a dependence on the polarization of the incident light, strong magnetic field generation, and a period of intense instability generation in the underdense plasma.

PACS numbers: 52.40.Nk, 52.35.Nx, 52.60.+h

The ongoing development of ultrabright, short pulse lasers is allowing exploration of new regimes of laser-matter interaction. Experiments are now being carried out [1–3] in which plasmas are irradiated by laser light with intensities up to $I\lambda_\mu^2 \simeq 10^{18}$ Wμm^2/cm^2. Here I is the intensity and λ_μ the wavelength in microns. At such intensities, electrons oscillating in the field of the light wave are strongly relativistic; i.e., $p_{os}/m_0c \geq 1$, where p_{os} is the momentum of oscillation, m_0 the electron mass, and c the velocity of light. This is the first simulation study to address an ultra-intense light wave with a finite spot size normally incident onto an overdense plasma-vacuum interface. Some of the key results are strong hole punching and MeV ion generation inward due to the large light pressure, MeV electron generation into the overdense plasma by nonadiabatic heating at the sharp light-plasma interface, and estimates for the absorption of the incident light and characteristic temperature of heated electrons for a range of laser intensities soon to be experimentally accessible.

We use a 2D, electromagnetic, relativistic electron, mobile ion, particle-in-cell code (ZOHAR [4]) to study this relatively unexplored, highly nonlinear regime [5]. As with previous 1D studies at lower intensities [6], these simulations model the interaction of laser light with a collisionless plasma. For the intensities and time scales studied here, inverse bremsstrahlung is weak since the light-plasma interface is quite steep and the effective temperature of the electrons interacting with the light wave is large. We begin with a simulation which focuses on the interaction of high-intensity laser light with a preformed, overdense plasma. Laser light with a Gaussian intensity profile (in the transverse or y dimension) is introduced at the left boundary and propagates (in the x direction) through a region of vacuum onto a slab of overdense plasma. Particles escaping through the right boundary are reemitted with their original temperature. In this example, the system is $36c/\omega_0$ long in the x direction and $40c/\omega_0$ wide, where ω_0 is the light-wave frequency. The plasma is initially $22c/\omega_0$ long, preceded by $14c/\omega_0$ of vacuum. The electric field of the incident light wave is in the y direction, and the dynamics are followed in the x-y plane (the so-called p-polarized case). In complementary simulations, the electric field is in the z direction (the s-polarized case). We consider both cases to provide insight into the three-dimensional aspects of the problem, which will be a mixture of the two cases. The initial density of the plasma slab is $4n_{cr}$, where n_{cr} is the critical density for the incident wave. The initial electron temperature Θ_e is 4 keV, and the electron-ion mass ratio is 1/1836. The incident wave is turned on over $72\omega_0^{-1}$ and has a Gaussian transverse intensity profile with half-width of $14c/\omega_0$, with a peak intensity of $I\lambda_\mu^2 = 1.2\times10^{19}$ Wμm^2/cm^2. This intensity corresponds to $p_{os}/m_0c = 3$.

The intense, linearly polarized light wave strikes the overdense plasma and penetrates a thin layer somewhat larger than c/ω_p due to the relativistic mass change [7]. (Here ω_p is the electron plasma frequency.) Even for normal incidence, there is a very strong, high-frequency electrostatic field operating on the plasma in this interface. This field is simply the oscillating component of the ponderomotive force [8] f_p; $f_p = \nabla(\gamma-1)m_0c^2$, where $\gamma = (1+p^2/m_0^2)^{1/2}$ and p is the electron oscillatory momentum in the transverse and longitudinal fields of the wave. Although generally nonresonant, this field can still accelerate electrons [9] which interact nonadiabatically with it in the steep interface. The frequency of the oscillating ponderomotive force is $2\omega_0$. This means that twice every cycle, a group of electrons will be accelerated into the plasma by this ponderomotive force. This will show up as a "train" of high-energy electrons, separated by a distance of half of a laser wavelength, or $\sim\pi c/\omega_0$. The heating is apparent in Fig. 1(a), which is a snapshot of p_x vs x of the electrons at $\omega_0 t = 180$. Figure 1(b) shows the energy spectrum of the heated electrons which have transported through the right boundary by $\omega_0 t = 400$. Note that these heated electrons have an effective temperature of about 1.1 MeV. At this time about 26% of the incident light-wave energy is being absorbed into these electrons.

Boring of the light beam into the plasma is a very important feature of the interaction. The light pressure p_L is extremely high; i.e., $p_L = 2I/c \sim 6\times10^3$ Mbar for, say, $I = 10^{19}$ W/cm^2. The hole punching is apparent in Fig. 2(a), which is a snapshot of the ion charge density at $\omega_0 t = 183$. As illustrated in Fig. 2(b), the depth of the

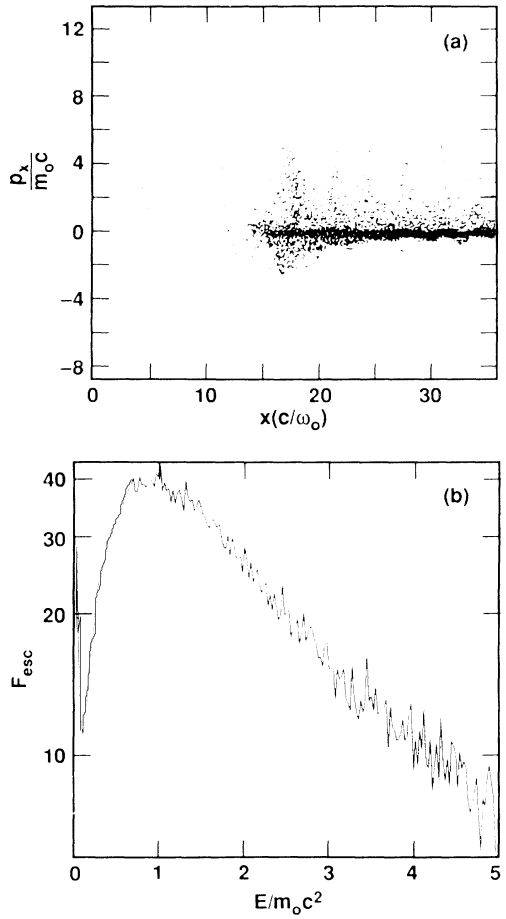

FIG. 1. (a) A snapshot of electron phase space (p_x vs x) at time $\omega_0 t = 180$ and (b) the cumulative energy distribution of the electrons striking the right boundary up to time $\omega_0 t = 400$. In this $2\frac{1}{2}$ D simulation, $p_{os}/m_0 c = 3$.

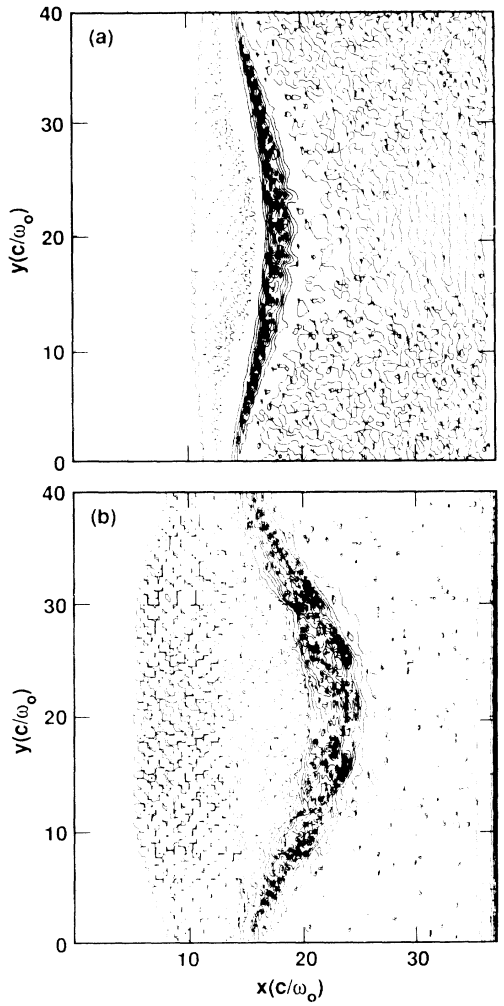

FIG. 2. Contours of the ion charge density at (a) $\omega_0 t = 183$ and (b) $\omega_0 t = 343$. The simulation parameters are the same as for Fig. 1.

hole increases with time. The depth increases with a velocity of about $0.022c$ in this example. This velocity can be estimated by balancing the momentum flux of the mass flow with the light pressure. In a frame moving with the velocity u of the reflection front, we use number and momentum conservation to obtain [10]

$$n_{pi} M u^2 = I/c \,. \tag{1}$$

Solving for the front velocity gives

$$\frac{u}{c} = \left(\frac{n_{cr}}{2n_{pe}} \frac{Zm}{M} \frac{I\lambda_\mu^2}{1.37\times 10^{18}} \right)^{1/2} . \tag{2}$$

Here n_{pi} (n_{pe}) is the ion (electron) plasma density, u the ion velocity, M the ion mass, and Z the charge state. For this example, Eq. (2) gives $u \simeq 0.025c$. More accurately, the momentum fluxes need to be described as second moments of a distribution, extending to about $c/30$ in this case. Note that this inward acceleration produces quite energetic ions, i.e., with energies $\sim 10^{-3} Mc^2$ in this example. This inward acceleration could be verified by observing a redshifting in frequency of the reflected light [3].

As the hole forms, the electric field of the light wave begins to directly drive the plasma electrons on the sides of the hole. As expected, the absorption efficiency increases. For example, at $\omega_0 t = 600$, the hole depth is about $1.5\lambda_0$, and the absorption efficiency into heated electrons has become about 50%. The energies of the heated electrons also increase. At $\omega_0 t = 600$, the effective temperature of the electrons transporting to the right is about 1.6 MeV. Note that previous studies [6,11] have concentrated on oblique incidence, whereas here we are normally incident with a finite beam width.

In other simulations with s-polarized light, the absorption and heated electron temperature were both somewhat reduced. In particular, for $I\lambda_\mu^2 = 1.4\times 10^{19}$ W μm^2/cm^2, the absorption at $\omega_0 t = 500$ was about 28% into heated electrons with a temperature of about 850 keV. Simulations were also carried out at a lower intensity of

$I\lambda_\mu^2 = 1.3\times10^{18}$ Wμm^2/cm^2. The absorption for p-polarized light was then about 20% into heated electrons with a temperature of about 290 keV. For s polarization, the absorption was about 10% into hot electrons with a temperature of about 140 keV. In addition, simulations with peak densities of $10n_{cr}$ gave no substantial change in the results.

Figure 3 summarizes the heated electron temperatures versus incident light intensity. The solid line is simply the energy (ϵ_p) of electrons oscillating in the transverse field of the incident light wave; i.e., $\epsilon_p = (\gamma_t - 1)m_0c^2$, where $\gamma_t = (1 + I\lambda_\mu^2/1.37\times10^{18})^{1/2}$. Note that ϵ_p is a simple scaling estimate and does not include the energy of oscillation in the longitudinal field, which would somewhat increase but greatly complicate the estimate. At low intensities, the hot electron temperature (say, due to resonance absorption) is typically much greater than ϵ_p. However, in this ultra-intense regime the absorption is occurring in a sharp interface. Hence it is plausible that ϵ_p provides a crude estimate for the characteristic heated energies.

Extremely intense self-generated magnetic fields are observed to form in the overdense plasma. Figure 4 shows contours of B_z at time $\omega_0 t = 600$ in the simulation with p-polarized light at $I\lambda_\mu^2 = 5.6\times10^{18}$ Wμm^2/cm^2. The periodic structure is associated with the incident and partially reflected light wave. Note the contours of the magnetic field inside the plasma. These contours represent a magnetic field around the heated spot in the center of the plasma. This nonoscillatory magnetic field is generated by the electron heating at the light-plasma interface. Here $eB_z/m\omega_0c \sim 1$, which corresponds to a field with magnitude $\sim$250 MG.

In addition to the sharply ramped overdense plasma-vacuum cases, we have carried out some $1\frac{1}{2}$ D simulations to allow the light to interact with a significant reigon of underdense plasma. Let us consider an example in which laser light with intensity $I\lambda_\mu^2 = 1.2\times10^{19}$ Wμm^2/cm^2 is propagated into plasma with an initial linear density profile rising from 0 to $4n_{cr}$ in a distance of $400c/\omega_0$. The initial electron temperature is 4 keV, and the electron-ion mass ratio is 0.01. In this case, the laser pulse is finite in length, and the plots we are about to describe are obtained after the laser has completely exited the system.

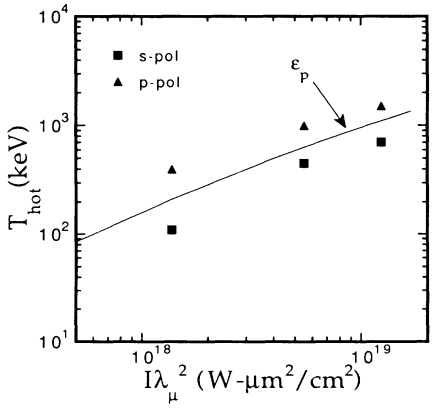

FIG. 3. The heated electron temperature vs intensity found in the $2\frac{1}{2}$ D simulations discussed in the text.

Again there is significant hot-electron generation due now to both the oscillating ponderomotive force heating near the critical density and the strongly driven Raman instability in the underdense plasma. This instability persists mainly near the quarter-critical surface due to the strong, self-consistent density modifications. In the electron phase space p_z vs x we observe large oscillations due to Raman scattered light at $\omega_0/2$ trapped in a local density modulation near $n_{cr}/4$. Hot-electron generation is also evident. In this $1\frac{1}{2}$ D example, about 50% of the light was absorbed into hot electrons with an effective temperature of about 800 keV. The reflected light was dominantly down-shifted to frequency $\omega_0/2$ in this example. At lower intensity ($I\lambda_\mu^2 = 1.3\times10^{18}$ Wμm^2/cm^2), only about several percent of the reflected light had frequency $\omega_0/2$.

In practice, lateral ejection of electrons from the laser beam spot reduces the efficiency of the underdense plasma instabilities. However, even for an expulsion velocity of 3×10^9 cm/sec, it would take a significant fraction of a picosecond to eject plasma from a 30-μm-diam spot. (Unless the density is quite low [12], the space charge prevents ejection of the electrons without the ions.) Hence, we expect interesting instability signals from experiments with ultra-intense, subpicosecond laser light.

Finally, we discuss the results obtained when a sizable region of underdense plasma is placed in front of an over-

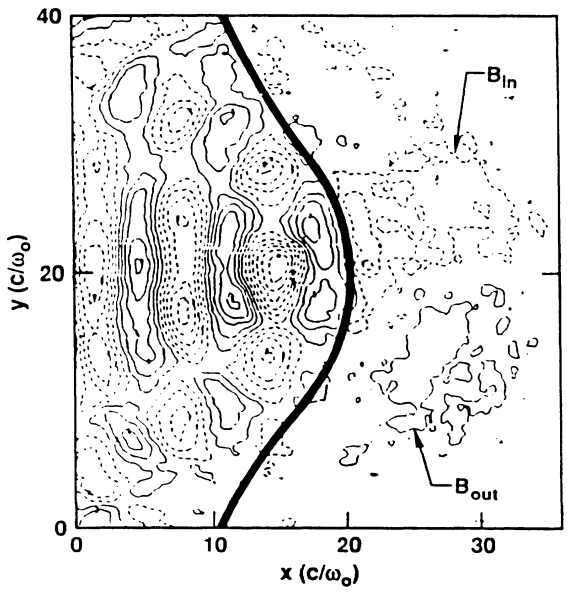

FIG. 4. Spatial contours of the magnitude of the magnetic field (B_z) at time $\omega_0 t = 600$. In this $2\frac{1}{2}$ D simulation, $p_{os}/m_0c = 2$.

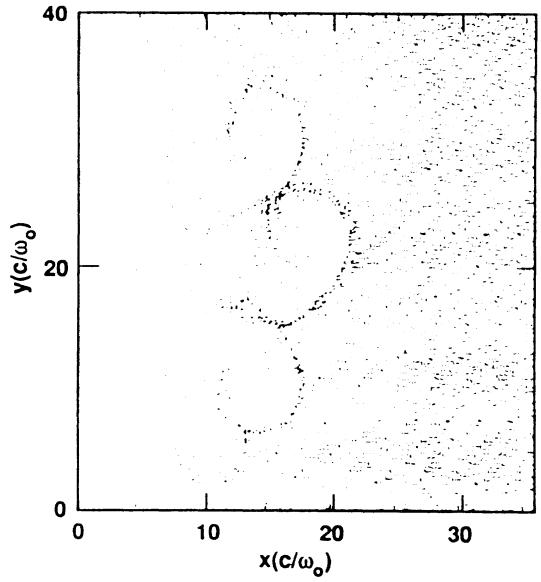

FIG. 5. Ion real space at $\omega_0 t = 800$ showing formation of bubbles near the critical surface. The central bubble eventually bores through the overdense plasma.

dense plasma slab in two dimensions. This is to illustrate how the combined effects from the underdense and overdense regimes already discussed can modify one another. These simulations begin with a plasma density that is ramped from 0 to $4n_{cr}$, over a distance of $4\lambda_0$, with an additional wavelength of plasma at $4n_{cr}$ behind the ramp. The incident laser parameters are identical to those discussed above, with a peak intensity of $I\lambda_\mu^2 = 5\times10^{18}$ W μm^2/cm^2, and is s polarized. As the laser light enters the system from the left and begins to penetrate through critical density, the surface of the plasma becomes corrugated (see Fig. 5). This behavior is related to the "bubble" formation studied previously by Valeo and Estabrook [13], as well as Lindman and Kindel *et al.* [14]. Our case differs in two respects: First, the pressure associated with the laser light is so intense that these bubbles are actually accelerated into the plasma; second, the perturbation on the critical surface is seeded by the electron motion in the underdense plasma well before the ions have a chance to move, in contrast to the previous work that assumes the ions to be responsible for the perturbations. This Rayleigh-Taylor-like instability is due to the photons effectively accelerating the plasma interface. As the pulse continues to propagate, the absorption increases as a function of time as the hole depth increases as discussed above. Other simulations, with various scale lengths of underdense plasma in front of supercritical plasmas, show similar behavior.

In summary, we have used particle-in-cell simulations to explore the interaction of ultra-intense laser light with plasmas. This has provided valuable insight into many complex features of this interaction. Most notably is hole boring, a crucial feature of the interaction, which leads to a time-dependent absorption and generation of very energetic electrons and ions directed into the overdense plasma.

We gratefully acknowledge useful conversations with K. Estabrook, W. B. Mori, J. M. Dawson, E. M. Campbell, J. Woodworth, J. Denavit, and C. Darrow. This work was performed under the auspices of the U.S. Department of Energy by the Lawrence Livermore National Laboratory under Contract No. W-7405-ENG-48.

[1] M. Chaker *et al.*, Phys. Fluids B **3**, 167 (1991); H. Milchberg *et al.*, Phys. Rev. Lett. **61**, 2364 (1988); O. L. Landen, D. G. Stearns, and E. M. Campbell, Phys. Rev. Lett. **63**, 1475 (1989).

[2] J. D. Kmetec *et al.*, Phys. Rev. Lett. **68**, 1527 (1992); A. B. Borisov *et al.*, Phys. Rev. Lett. **68**, 2309 (1992).

[3] D. Umstadter *et al.*, in *OSA Proceedings on Short-Wavelength Coherent Radiation*, edited by P. H. Bucksbaum and N. M. Ceglio (Optical Society of America, Washington, DC, 1991), Vol. 11, pp. 276 and 280.

[4] A. B. Langdon and B. F. Lasinski, in *Methods in Computational Physics*, edited by J. Killeen, R. Alder, S. Fernbach, and M. Rotenberg (Academic, New York, 1976), Vol. 16, p. 327.

[5] W. Priedhorsky *et al.*, Phys. Rev. Lett. **47**, 1661 (1981); D. R. Bach *et al.*, Phys. Rev. Lett. **50**, 2082 (1983).

[6] P. Gibbon and A. R. Bell, Phys. Rev. Lett. **68**, 1535 (1992).

[7] P. Kaw and J. Dawson, Phys. Fluids **13**, 472 (1970).

[8] P. Sprangle, E. Esary, and A. Ting, Phys. Rev. Lett. **64**, 2011 (1990); C. J. McKinstrie and D. F. DuBois, Phys. Fluids **31**, 278 (1988); W. B. Mori *et al.*, Phys. Rev. Lett. **60**, 1298 (1988).

[9] W. L. Kruer and K. G. Estabrook, Phys. Fluids **28**, 430 (1985).

[10] W. L. Kruer, E. J. Valeo, and K. G. Estabrook, Phys. Rev. Lett. **35**, 1076 (1975).

[11] F. Brunel, Phys. Rev. Lett. **59**, 52 (1987); Phys. Fluids **31**, 2714 (1988); G. Bonnaud, P. Gibbon, J. Kindel, and E. Williams, Laser Part. Beams **9**, 339 (1991); K. G. Estabrook and W. L. Kruer, Lawrence Livermore National Laboratory Annual Laser Program report, 1986 (unpublished).

[12] Guo-zheng Son, Edward Ott, Y. C. Lee, and P. Guzdar, Phys. Fluids **30**, 526 (1987).

[13] E. J. Valeo and K. G. Estabrook, Phys. Rev. Lett. **34**, 1008 (1975); Kent Estabrook, Phys. Fluids **19**, 1733 (1976).

[14] E. L. Lindman, J. Phys. (Paris), Colloq., Suppl. 12, **38**, C6-9 (1977); J. M. Kindel *et al.*, U.S. Seminar on Theory and Application of Multi-Ionized Plasmas Produced by Laser and Particle Beams, Nara, Japan, 3–7 May 1982 (unpublished).